PAPER

Effect of grain refinement on material properties of Mg-8%Al-0.5%Zn alloy after the combined processes of multi-direction forging and equal channel angular pressing

Recent citations

- Effect of Annealing and Aging Treatment on Pitting Corrosion Resistance of Fine-Grained Mg-8%Al-0.5%Zn Alloy
Gajanan M. Naik *et al*

To cite this article: Gajanan M Naik *et al* 2019 *Mater. Res. Express* **6** 096538

View the article online for updates and enhancements.

This content was downloaded from IP address 157.49.106.22 on 29/09/2020 at 07:50

Materials Research Express

PAPER

Effect of grain refinement on material properties of Mg-8%Al-0.5%Zn alloy after the combined processes of multi-direction forging and equal channel angular pressing

RECEIVED
25 May 2019

REVISED
19 June 2019

ACCEPTED FOR PUBLICATION
28 June 2019

PUBLISHED
10 July 2019

Gajanan M Naik[1], **B N Anjan**[2], **Narendranath S**[1], **S Satheesh Kumar S**[3] **and Preetham Kumar G V**[2]

[1] Corrosion Engineering Laboratory, Dept. of Mechanical Engineering, NITK, Surathkal, 575025, Mangalore, Karnataka, India
[2] Dept. of Metallurgical and Materials Engineering, NITK-Surathkal, 575025, Mangalore, Karnataka, India
[3] Defence Metallurgical Research Laboratory, Hyderabad 500058, Telangana, India

E-mail: gajamnaik@gmail.com

Keywords: AZ80, MDF, ECAP, UFG, corrosion

Abstract

Establishing the novel microstructure is an effective method to accelerate the applications of magnesium and its alloys. In this work, an Mg-8%Al-0.5%Zn alloy (AZ80 Mg) with ultra-fine-grain (UFG) size of ~1.29 μm was achieved by the combined processes of multi-directional forging (MDF) and equal channel angular pressing (ECAP). The achieved ultra-fine grain structure made the Mg alloy, owing to inclusive performance as the structural material. The AZ80 Mg alloy with MDF 6 pass followed by two pass ECAP has superior mechanical properties such as ultimate tensile strength (UTS) of 352 MPa and elongation of 11% when compared to as-received Mg alloy. Also, an unprocessed Mg alloy showed the corrosion rate of a 13.28 mm y^{-1}, the corrosion rate of processed Mg alloy could be further decelerated through a change of microstructure obtained from combined processes of MDF and ECAP. This study outstandingly obtained a 94% reduction of corrosion rate after MDF-3P followed by an ECAP-2P (0.77 mm y^{-1}) process compared to as-received Mg alloy.

1. Introduction

Magnesium alloys are considered as potential material for automobile, marine, electronic and aerospace industries due to their low weight density and high specific strength. However, the mechanical properties such as hardness, tensile strength and ductility of them are comparatively less associated with another category of engineering materials. Along with this Mg alloys have lower corrosion resistance properties in corrosion media and this hinders the use of Mg alloys in various structural applications [1]. The industrial applications of Magnesium alloys are further improved by the enhancement of their mechanical and corrosion behaviour using severe plastic deformation (SPD) technique. The SPD technique adapted to achieve ultra-fine-grain structure, thereby increasing mechanical performance and corrosion resistance. In particular, MDF and ECAP are a promising technique to attain UFG structure. MDF is one of the most capable methods to accomplish fine-grain structure in bulk materials. MDF involves repeated compression on the specimen, changing the axis to 90° in every pass [2–4]. The effect of MDF on microstructure and mechanical properties of Mg alloys was reported. Qingfeng *et al* [5] have examined the effect of MDF on AZ80 Mg alloy by decreasing processing temperature from 683 K to 573 K, as a result, the grain size decreases with increasing the accumulative strain at a lower temperature. Hong *et al* [6] explored the effect of MDF on microstructure, texture and mechanical properties for Mg-7Gd-5Y-1Nd-0.5Zr. Study exhibited the maximum ductility of 21% at 470 °C which was showing a 200% improvement when compared with that of the solutionized specimen, this is due to refined fine grains as well as the weakened texture during the process. Salandari *et al* [7] examined the microstructure and mechanical behaviour of an MDF processed WE Mg alloy, the investigation showed an increased volume fraction of recrystallized grains with respect to MDF cycles and achieved a mean grain size of 4.8 μm after 5-MDF passes. Additionally, led to a combined enhancement in UTS and % elongation of 460 MPa and 12% respectively.

© 2019 IOP Publishing Ltd

Huang *et al* [8] observed the significant enhancement of mechanical properties after MDF. With the increase of MDF passes for AZ31 Mg alloy. Jinlong *et al* [9] showed that AZ80 Mg alloy was effectively refined through high-pass multi-directional forging, and mean grain size was reduced to 0.73 μm after 24 passes of forging. Its ultimate tensile strength, yield strength and % elongation reached 333.8 MPa, 233.7 MPa and 17.8%, respectively, which were 1.22 times, 1.35 times and 2.54 times of those before the forging.

The ECAP is another most popular SPD method since they are capable of producing uniform fine-grained microstructures in materials without changing the shape of the sample. The formation of the microstructure is due to the existence of dynamic recrystallization (DRX) mechanism and by the parameters of ECAP, such parameters are die angle (ϕ), corner angle (ψ), processing temperature, ram speed, and the processing route. The effect of these ECAP parameters on the grain size and the mechanical properties and corrosion behaviour has been explored for various Mg alloys [10, 11]. Muralidhar *et al* [12] observed the influence of ECAP processing temperature on grain size and mechanical properties of AZ61 alloy as a result, the mean grain size of the AZ61 specimen was found to be decreased to 85.0%, 81.0% and 70.0% for the extrusion temperatures of 210 °C, 250 °C and 300 °C respectively. Further, the tensile strength of the Mg alloy increased by 24%, 10% and 12% for the extrusion temperatures of 210 °C, 250 °C and 300 °C respectively. Gopi *et al* [13] have investigated the wear and corrosion behaviour of AM70 Mg alloy by ECAP process. From the study, it was noticed that there is an improvement in wear and corrosion resistance of ECAP processed AM70 alloy, this is due to the grain refinement and uniform distribution of secondary phases. Zhou *et al* [14] observed the microstructure and mechanical properties of WE43 after ECAP. The result showed that the mean grain size significantly decreased from ~50 μm to ~1.5 μm through ECAP for 4P with homogeneous microstructure. The investigation also reported that the ductility of ECAP processed WE43 alloy increased from 1–4P then decrease from 4–12P, this is due to strong basal texture (0002). Qiyu *et al* [15] proposed that the secondary extrusion process could strongly refine the recrystallized grains and disperse the fine RE-containing phases in AZ80 Mg alloy. The % elongation of the AZ80RE Mg alloy was also improved, due to the fine grain structure and the basal texture weakening. Lei *et al* [16] demonstrated that as-extruded Mg-Zn-Zr lead to compressive strength improvement. The improved strength of the Mg alloy was predominantly attributed to the grain refinement and dispersion strengthening of nano-MgO particles and $MgZn_2$ particles. Besides, a comparative study of MDF and ECAP processed for microstructure evolution and precipitation of phases was reported. Heczel *et al* [17] have made a comparative analysis of the microstructural analysis in Mg-6Al-0.5Mn alloy processed by ECAP and MDF. The study revealed that the much greater dislocation density and the precipitate fraction was observed for ECAP-2 passes when compared to MDF processed material. Shakhova *et al* [18] studied the microstructure evolution of MDF and ECAP to a strain of ~4 times, obtained an ultra-fine grain structure in a Cu-0.3Cr-0.5Zr alloy with a mean grain size of 0.60 μm and 1.10 μm respectively. MDF is capable to accomplish faster kinetics of grain size reduction as compared to ECAP. Therefore, the effect of the combined processes of MDF and ECAP on microstructures, mechanical and corrosion behaviour of AZ80 Mg alloy has a pronounced significance. Although, combined processing of MDF and ECAP technique has not been reported yet in sufficient detail. The graphical abstract of combined processed by MDF + ECAP as shown in figure 1.

The current work provides the evolution of microstructure, mechanical properties and corrosion resistance in AZ80 Mg alloy as a function of MDF followed by ECAP. In addition, this work examines the effect of the grain size and secondary phase on responses was observed and discussed.

2. Materials and experimental work

As-received AZ80 Mg alloy supplied by Exclusive Magnesium Pvt. Ltd. Hyderabad, India, with an elemental composition of Al (8%)-Zn (0.5%)-Mg (Balance) was used in the current work. Microstructure and EDS results of the as-received alloy have shown in figure 2. After diffusion annealing at 400 °C for 24 h, samples with 30 × 30 × 25 mm dimension were prepared by conventional machining. Subsequently, samples were processed through multi-directional forging at 325 °C up to 3 Pass (1 cycle) and 6 Pass (2 cycles). A sample must be deformed in all three directions for 3 numbers of passes to complete one cycle as shown in figure 1. Further, the MDF processed samples were turned to 16 mm diameter and 30 mm length and processed by ECAP two passes at 325 °C under a ram speed of 1 mm s^{-1} with a die channel angle 110°, 30° corner angle and processed by route R method. The microstructure of the unprocessed and processed AZ80 Mg alloy was observed by optical microscopy (OM; BIOVIS material plus), scanning electron microscopy (SEM; JEOL JSM 6380LA) and JEOL JSM-7100F FESEM equipped with electron backscattered diffraction (EBSD) detector. Presence of primary and secondary phases and to analyze the change of orientation in processed samples was explored through X-ray diffraction analysis (XRD; PROTO– iXRD MGR40). The scanning angle range was 20°–90° and the scanning speed was 2 °/min with a target material of Cu Kα. The mechanical properties of the processed and unprocessed samples were measured by a Shimadzu universal testing machine (UTM; AG–X plus TM100 kN). The

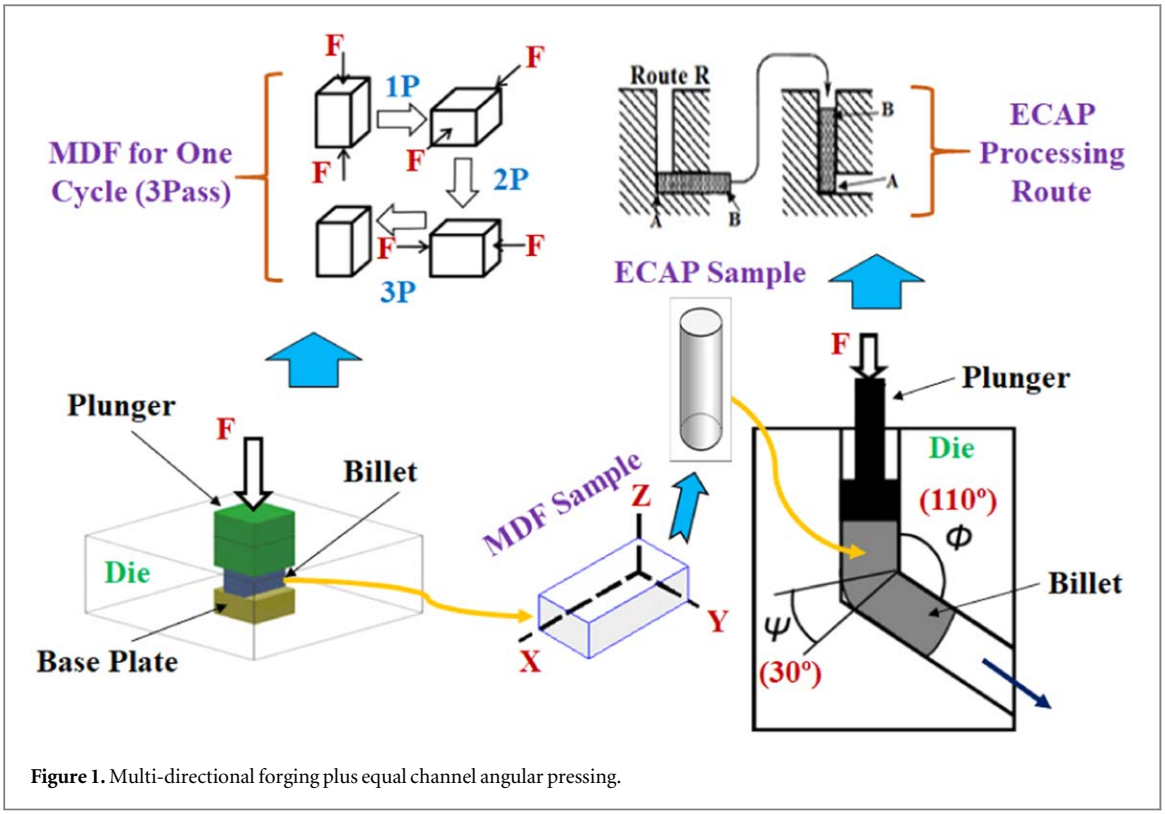

Figure 1. Multi-directional forging plus equal channel angular pressing.

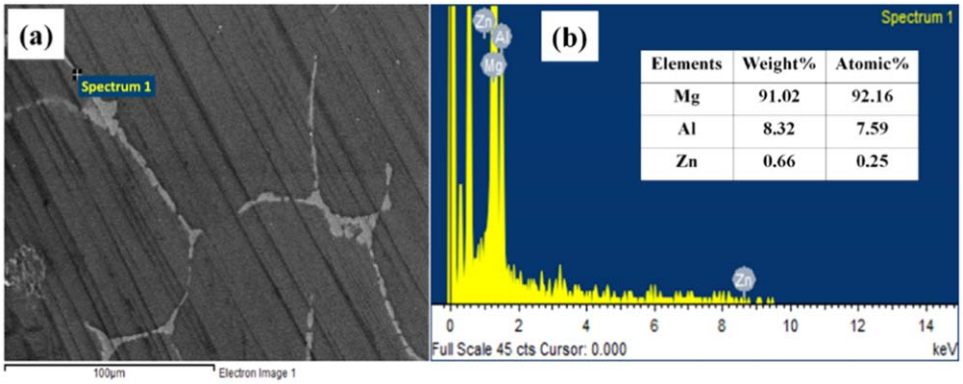

Figure 2. SEM micrograph with EDS results of AZ80 Mg alloy.

Microhardness test was conducted at a load of 100 g with a dwell time of 13 s. The corrosion behaviour of processed and un-processed AZ80 Mg alloys was investigated by electrochemical corrosion analyzer; Model: Gill AC-1845. The potentiodynamic polarization was performed in 3.5 wt% NaCl solution. The auxiliary electrode (AE)—Graphite (Gr) and the reference electrode (RE)-saturated calomel electrode (SCE). 1 cm^2 area of the working electrode (AZ80 alloy) was exposed to the 3.5 wt% NaCl solution. Potentiodynamic polarization tests were conducted using a scan rate of 2 mV s^{-1} and a scan range of −200 mV to +200 mV.

3. Results and discussion

3.1. Microstructural observations

Figures 3 and 4 shows OM and SEM images of the processed and unprocessed AZ80 Mg alloys. It was observed that the as-received and SPD processed Mg alloys essentially consists of the α-Mg primary phase and β-$Mg_{17}Al_{12}$ secondary phase at the grain boundaries which is as shown in figure 3(a). Additionally, which was significantly addressed in our previous article [19]. Also, the XRD (figure 7) and EDS analysis (figure 2) of the as-received Mg alloy shows the presence of secondary phases and elemental compositions respectively. Figures 3(b), (d) presents the optical images of AZ80 Mg alloy after ECAP-2P, MDF-3P and 6P at 325 °C respectively. It is observed that

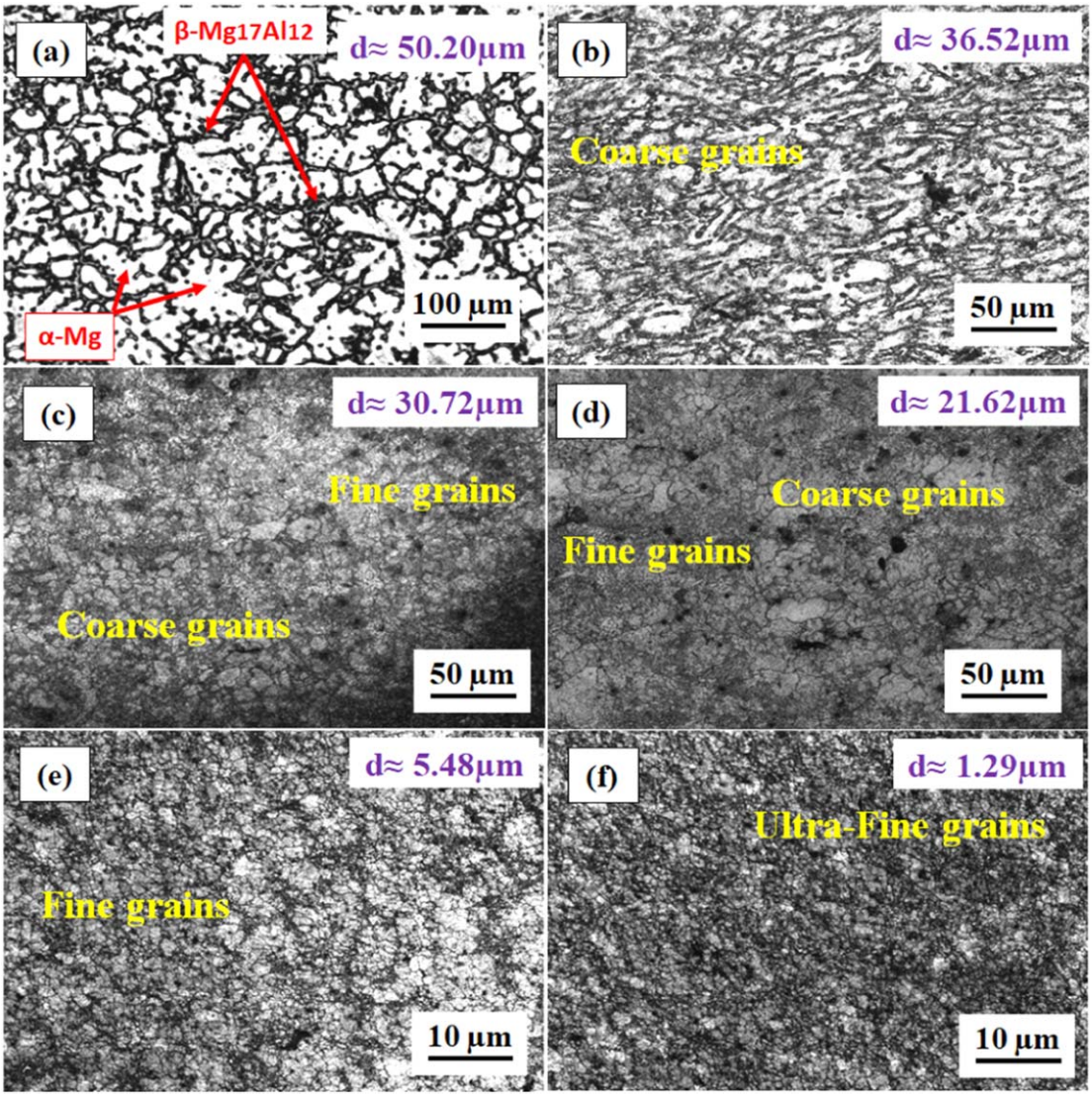

Figure 3. Optical images of AZ80 Mg alloys (a) As-received (b) ECAP-2P (c) MDF-3P (d) MDF-6P (e) MDF-3P + ECAP-2P (f) MDF-6P + ECAP-2P.

the microstructure of the Mg alloys predominantly elongated and refined from original grains due to dynamic recrystallization process (DRX) [20]. Also, the microstructure composed of bimodal grains, here coarse grains are surrounded by finer grains, but coarse grains occupy a larger area fraction during ECAP-2P this is due to insufficient slip systems of HCP crystal structure [21] and the achieved critical average grain size of about ~36.52 μm. During MDF-3P and 6P obtained fine-grained microstructure with a mean grain size of ~30.72 μm and ~21.62 μm respectively, this improved grain refinement mainly due to the increased number of MDF passes. Poggiali *et al* [22] explored the effect of the combined processes of rolling + ECAP on microstructure evolution and discussed the effect of the initial grain size of magnesium and its significance in his paper. According to Poggiali *et al* Initial grain size has significant influence to achieve further grain refinement during ECAP. Therefore, the use of the combined processes of an ECAP after an intermediate step of MDF or vices-versa simplifies grain refinement and leads to homogeneous and uniform grain structure. These have been evidently proved in our study as shown in figures 3(e) and (f). Indeed, figures 3(e) and (f) illustrates the microstructure of MDF 3P followed by ECAP-2P specimen and MDF 6P followed by ECAP-2P at 325 °C through route R respectively. The combined processes have shown ultra-fine grains and more uniformly distributed structure of mean grain size of ~1.29 μm. The achieved ultra-fine grained alloy after combining MDF and ECAP processes produce large grain boundaries in the bulk material. Moreover, β-$Mg_{17}Al_{12}$ secondary phases were isolated at the grain boundaries in as-received Mg alloys, and also observed a non-uniform distribution of secondary phases, a similar observation made by Guangwei *et al* [23] while combined processing of ECAP, Rolling and electro pulsing treatment (EPT) of Mg alloy. When secondary phases have been exposed to the different plastic strains while processing with SPD may break the large secondary phases into

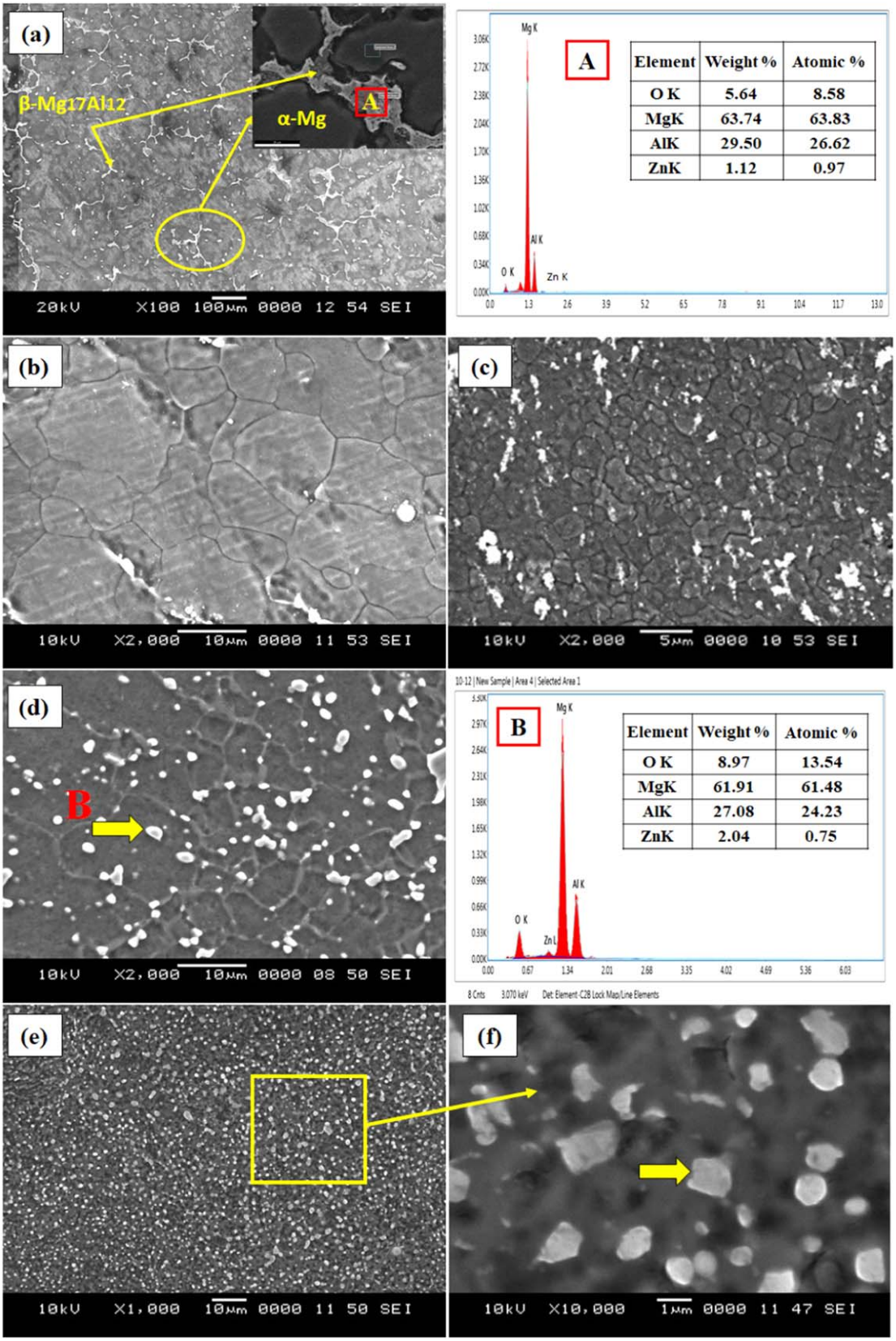

Figure 4. SEM images of AZ80 Mg alloys (a) As-received with EDS analysis of the secondary phase marked as A (b) MDF-6P (c) MDF-6P + ECAP-2P (d) Distribution of secondary phase in MDF-6P with EDS analysis marked as B (e), (f) Dispersed secondary phase in MDF-6P + ECAP-2P sample.

small fragments and precipitated in the Mg matrix. Meanwhile, by the combined processes of MDF followed by ECAP may also promote the growth of the precipitates of secondary phases. Therefore the area fraction of micro galvanic cells between α-Mg phase and β-$Mg_{17}Al_{12}$ secondary phase was reduced, which cause a slowdown in

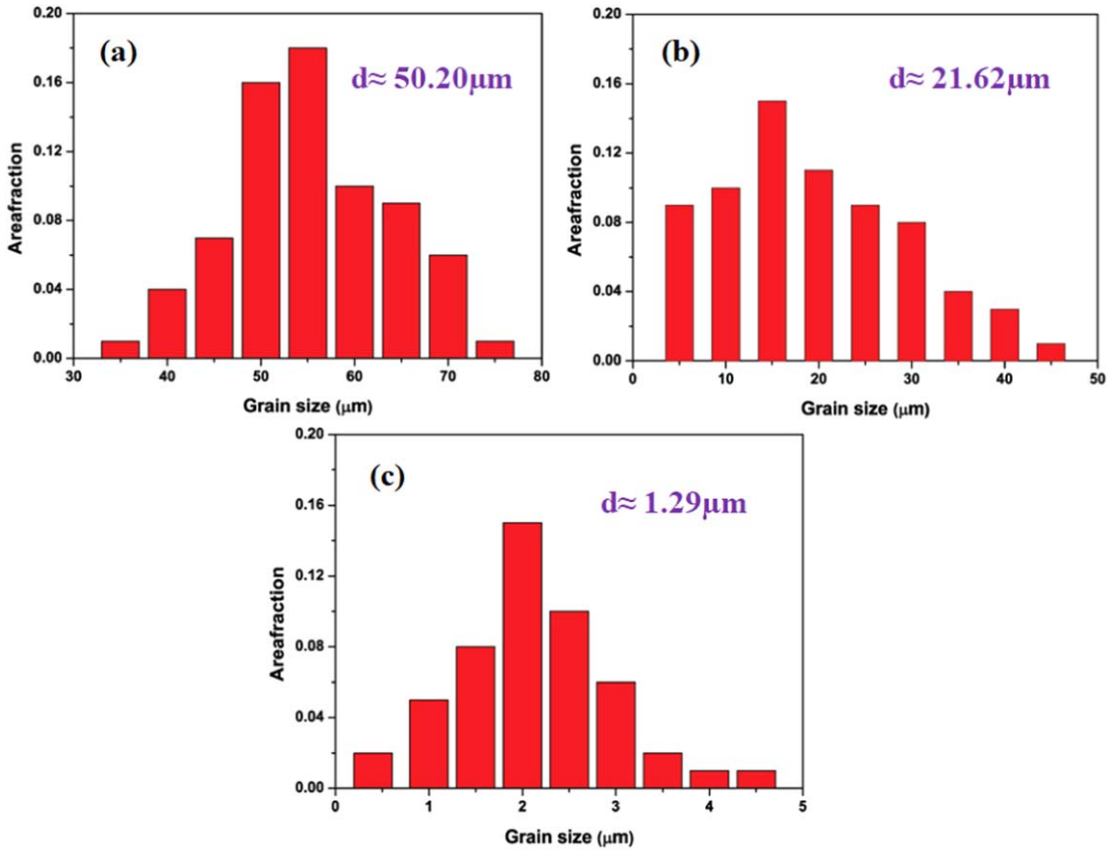

Figure 5. Grain size distribution of AZ80 Mg alloys (a) As-received (b) MDF-6P (c) MDF-6P + ECAP-2P.

the corrosion rate this mechanism was evidently discussed in the upcoming sections. Also, grain refinement could excellently enhance the mechanical properties of Mg alloys agreeing to the Hall–Petch theory [24, 25]. The SEM micrographs in figure 4 displays bright and dark field images for the AZ80 Mg alloy before and after SPD processes. Measurement gives an average grain size of as-received Mg alloy of ~50.20 μm in figure 4(a) but the grain distribution was non-uniform. The grains are refined and homogeneous in AZ80 Mg alloy in figures 3(b)–(d) after processing with MDF and ECAP. However, the grain refinement and distribution of secondary phases were most effective in Mg alloy with MDF-6P and combined processes of MDF followed by ECAP shown in figures 4(b) and (c) which measures a mean grain size of ~21.62 μm and ~1.29 μm for MDF-6P and MDF-6P + ECAP-2P respectively. Along with this figure 5 contributes the grain size distributions of the SPD-processed Mg alloys for three different specimens being summarized. It is apparent that the average grain size of the samples is reduced significantly by combining two SPD processes such as MDF and ECAP. Figures 4(d)–(f) shows the SEM micrographs of the MDF-6P and MDF-6P + ECAP-2P samples. It is observed that secondary phases (β-$Mg_{17}Al_{12}$) dispersed inside the grains displayed by the arrows: point B in figure 4(d). The marked β-$Mg_{17}Al_{12}$ have all of the alloying elements (i.e. Mg, Al and Zn) as analyzed by EDS analysis of the MDF-6P specimen and also it has been further confirmed by X-ray diffraction analysis. Figures 4(e), (f) presents the uniform distribution of the secondary phase (β-$Mg_{17}Al_{12}$) inside the grains of the MDF-6P + ECAP-2P specimen. From this, it is evident that secondary phase particles distributed in the α-Mg matrix as the SPD passes progressed.

3.2. EBSD analysis

Figure 6 shown the EBSD map of the as-received and SPD processed specimens. The EBSD study evidently revealed that the 2P- ECAP Mg alloy was composed of the coarse grains with a mean grain size of 36.52 $\pm$ 2.9 μm, which was lesser than that of the as-received alloy (50.20 μm). Also, the microstructure of AZ80 Mg alloy consists of ultra-fine grains, occurred by DRX, with only a few elongated grains after combined processes of MDF-6P followed by ECAP-2P as shown in figure 6(c). Combined processing of MDF-6P + ECAP-2P yielded a mean grain size of ~1.29 $\pm$ 0.7 μm as revealed in the EBSD map in figure 6(c) with consistent grain size distribution in figure 6(f). The grain size distribution displays a large variation in the mean grain size with the number of SPD passes (figure 6). After the second pass ECAP, the effective variation in mean grain size is minor shown in figure 6(e). However, a significant modification in the grain size reduction has been

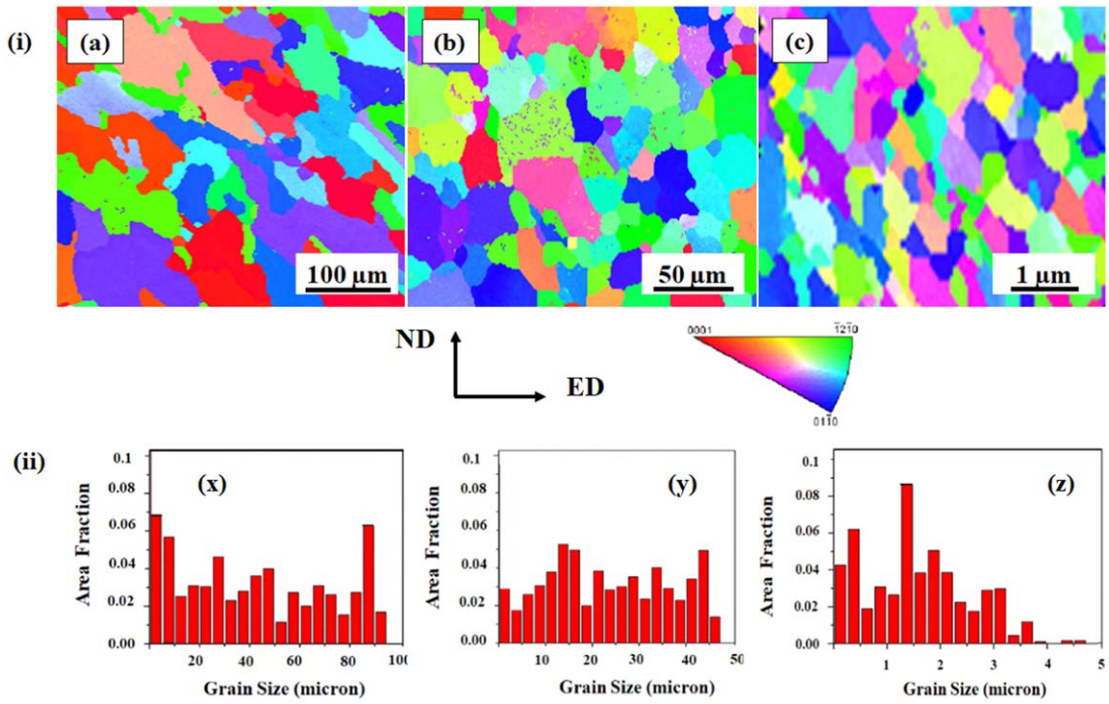

Figure 6. EBSD based analysis of SPD processed AZ80 Mg alloys (i) (a) As-received (b) ECAP-2P (c) MDF-6P + ECAP-2P (ii) Grain size distribution for (x) As-received (y) ECAP-2P (z) MDF-6P + ECAP-2P.

observed with the combined process of MDF and ECAP. Hence, it indicates that combined processing of MDF + ECAP promotes a substantial grain refinement in AZ80 alloy via DRX mechanism [17]. It is remarkable that such a noteworthy grain refinement can also be attributed to the initial grain structure of AZ80 alloy meanwhile the initial microstructure of the Mg alloys plays a critical role in the improvement of grain refinement and in determining the final grain size after MDF + ECAP. Initial grain size can simplify the grain refinement process in AZ80 Mg alloys owing to the high density of grain boundaries.

3.3. X-ray diffraction analysis

The microstructure of AZ80 alloy is more consistent with the X-ray diffraction results, α-Mg and β-$Mg_{17}Al_{12}$ phases existing in alloying as-received and SPD processed AZ80 alloy as shown and marked in figure 7. The AZ80 Mg alloy rich in β-$Mg_{17}Al_{12}$ secondary phases due to the presence of high aluminium content in the matrix [26]. Also, secondary β-phases were segregated along the grain boundaries in the as-received alloy, which is evidently observed and reported through OM and SEM images with EDS results which are depicted in figures 3(a) and (a) respectively. In addition, Mg alloys processed through SPD exhibited a more uniform and homogeneous distribution of secondary phases. Consequently, the peak intensity of Mg alloy was increased relative to the as-received Mg alloy. From figure 7, it was observed that SPD processed Mg alloys showed higher intensity peaks due to the high volume fraction of secondary phases after process [27], which is evident from microstructure evolution of processed and unprocessed sample shown in figures 3 and 4(d)–(f).

3.4. Microhardness

The microhardness variations in AZ80 Mg alloys after different SPD passes presented in figure 8. It is revealed that the microhardness was increased with the increase in equivalent plastic strain after each SPD pass. As the number of SPD passes increases for both individual and combined processes of SPD leads to increasing microhardness due to grain refinement, strain hardening and distribution of secondary phases [28]. Microhardness of the ECAP-2 pass Mg alloys is 70 Hv. During MDF-3P and MDF-6P, the microhardness was 83 Hv and 84 Hv which shown a rise in microhardness compared to ECAP-2P processed alloy this is due to increased plastic strain during the process [29].

The MDF-3P + ECAP-2P and MDF-6P + ECAP-2P process hardness values are 86 Hv and 89 Hv respectively. During combined processes of MDF followed by ECAP, the grain refinement increased dislocation density in the Mg bulk material due to induced plastic strain and also due to the uniform distribution of secondary phases lead to improved hardness [30]. Therefore, the microhardness of magnesium alloy became higher than that of the as-received and primarily SPD processed Mg alloys. Particularly, after ECAP-2P

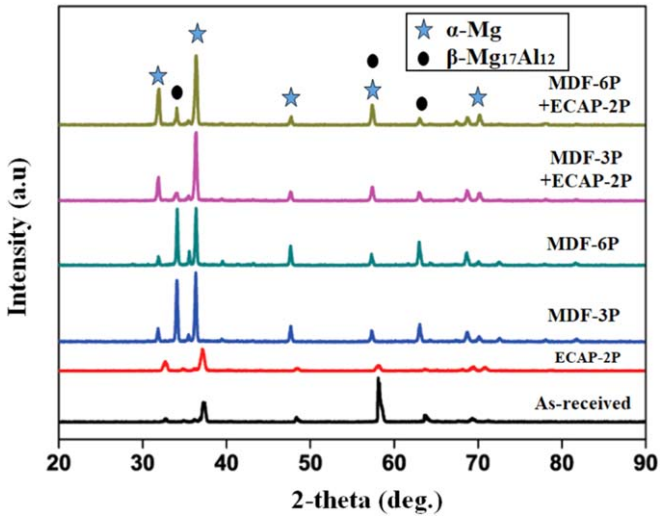

Figure 7. X-ray diffraction pattern for processed and unprocessed AZ80 Mg alloys.

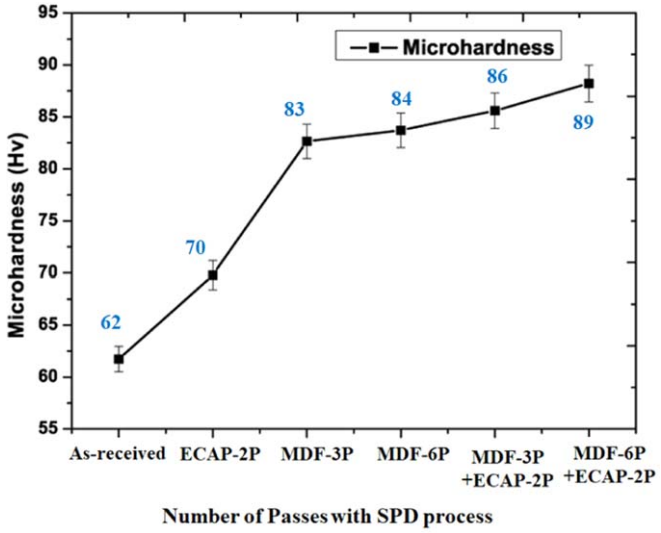

Figure 8. Microhardness variation of AZ80 Mg alloys after the SPD process.

extrusion at 325°C, the microhardness increased by 12%. After MDF-6P + ECAP-2P process the microhardness increased by 30%.

3.5. Tensile strength

Figure 9(a) illustrates the engineering stress-strain curves (b) variation of the ultimate tensile strength (UTS), yield strength (YS) and % elongation of AZ80 Mg specimens corresponding to as-received, ECAPed, MDF processed and MDF followed by ECAPed. From this study, it is evident that as-received alloy processed through SPD at elevated-temperature increases the YS, UTS and ductility of the Mg alloy. However, the continues shearing and grain refinement through MDF followed by ECAP process simultaneously increase both strength and ductility of the Mg alloy. Initially, as-received Mg alloy showed a lower percentage of elongation, YS and UTS of about 3.2%, 168 MPa and 189 MPa respectively. However, after processing with ECAP-2P and MDF-3P the strength and ductility were improved instantaneously shown in figures 9(a) and (b). The UTS and % elongation for Mg alloys processed at 325 °C up to 6-Pass MDF is 305 MPa and 8.22%, respectively. This is due to grain boundary strengthening and strain hardening effect [31]. Further, Multi-directional forged Mg alloys up to 3 and 6 passes, subjected to ECAP up to 2 passes. These samples tensile behaviour were observed and shown in figure 8. From, figure 9 it is revealed that the MDF-3P + ECAP-2P and MDF-6P + ECAP-2P shown the complete enhancement of strength by increasing ductility. This is due to obtained homogenous fine-grains and distribution of secondary phases achieved in the alloy. Indeed, the tensile behaviour of the AZ80 Mg alloy after

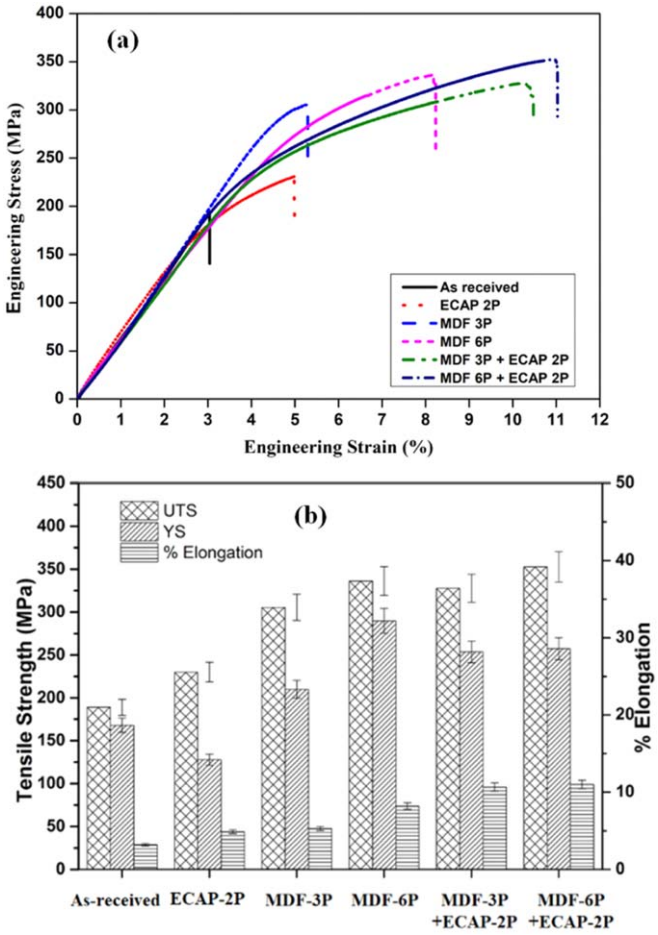

Figure 9. (a) Engineering stress versus engineering strain and (b) UTS, YS and percentage elongation for various SPD pass of AZ80 Mg alloys.

ECAP and MDF exhibits lower tensile strength and ductility compared to Mg alloy processed by MDF + ECAP. Hence, obtained results suggest that MDF + ECAP processing improves the tensile strength and % elongation of the Mg alloys. However, the microstructure illustrates that the combined processes of MDF + ECAP processing lead to an ultra-fine grain structure. Therefore, the above desired mechanical properties were achieved after MDF followed by ECAP must be attributed to texture effects [32].

3.6. Fractography

Figure 10 presents the SEM morphologies of the fractured surfaces of the as-received and SPD processed specimens. The fracture surfaces of all the samples resulted in cleavage morphology, which specifies that the fracture continued with less dislocation slip systems, indicating the brittleness of the examined alloy. Also, failure surfaces consist of small dimples and cracks. Brittle fracture mainly observed in the as-received alloy due to the presence of undissolved brittle secondary phases in the bulk material shown in figure 10(a). Furthermore, interdendritic porosity was observed on the fractured surfaces of Mg alloys which lead to decreased ductility as presented in figures 10(a)–(c). The changes in the fracture behaviour between the coarse grain structured samples such as as-received, ECAP-2P, MDF-3P and a fine grain Mg alloy of MDF-6P and combined SPD processed Mg alloy can be seen from the SEM fractographs in figures 10(a)–(f). Certainly, some dimples, cleavage together called quasi-cleavage fracture and tear ridges were observed on the surface of fine and ultra-fine grained samples which results in the enhancement of ductility as depicted in figures 10(e) and (f) [33]. The MDF + ECAP processed samples showed ductile behaviour with a higher fraction of dimpled structure when compared with other specimens. The obtained fractography has good agreement with the engineering stress-strain curves depicted in figure 9.

3.7. Potentiodynamic polarization

As per literature and based on our obtained results, the two factors appear to play the utmost significant role in the corrosion resistance of Mg alloys, such as grain boundaries and secondary phases ($Mg_{17}Al_{12}$). Their role is

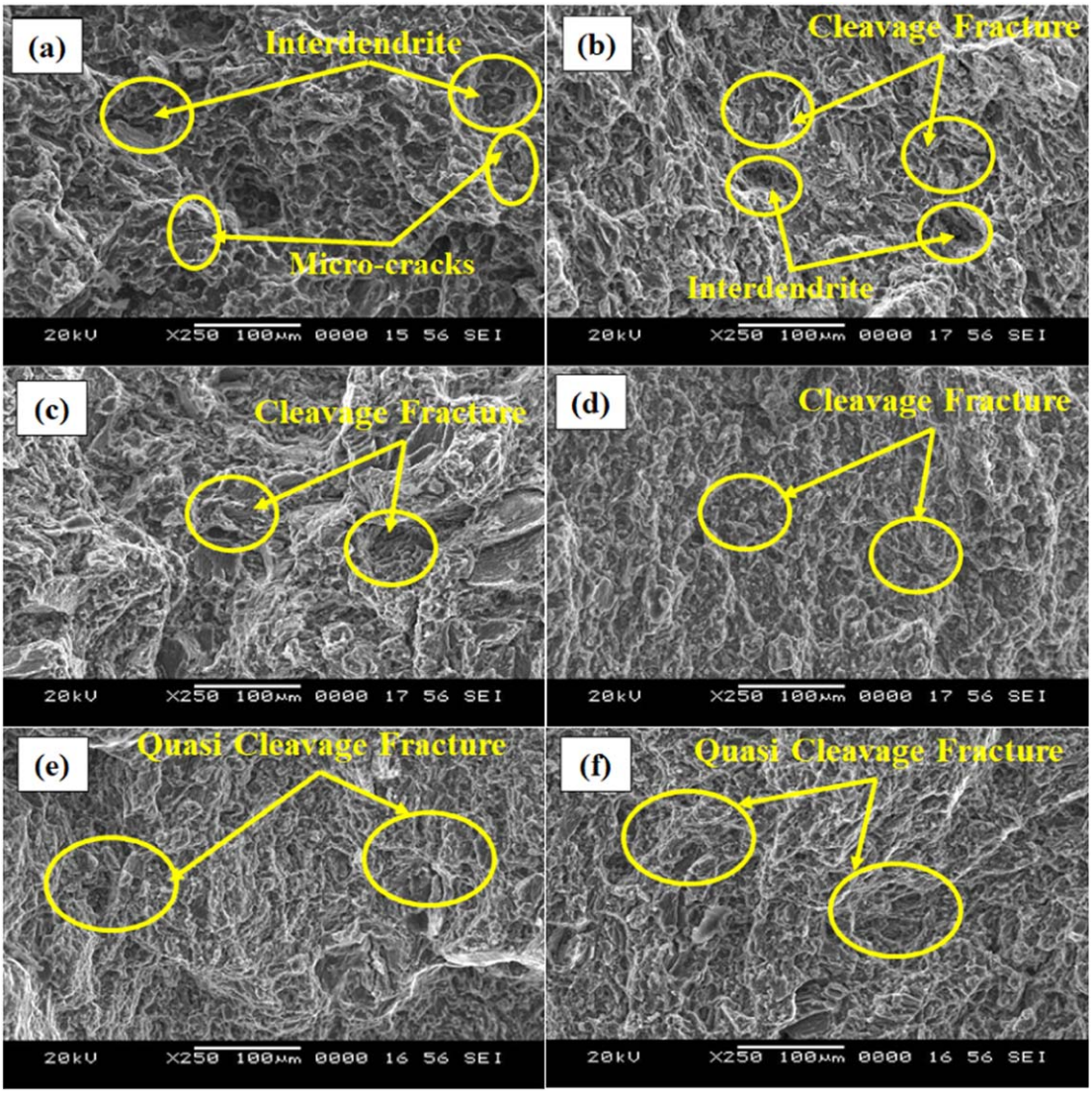

Figure 10. Fractography of AZ80 Mg alloys (a) As-received (b) ECAP-2P (c) MDF-3P (d) MDF-6P (e) MDF-3P + ECAP-2P (f) MDF-6P + ECAP-2P.

discussed in detail in the context of the outcome of the current investigation. During this study the attempt is made to achieve very large grain boundaries and uniform distribution of secondary phase particles by combining two SPD processes such as MDF and ECAP, as a result, MDF-3P + ECAP-2P and MDF-6P + ECAP-2P produce average grain size of ~5.48 μm and ~1.29 μm respectively and results were discussed in the above sections in detailed with figures 3 and 4. Better pitting corrosion resistance was achieved after combined processes of MDF and ECAP and the obtained polarization results are correlated with the grain boundaries and β-$Mg_{17}A_{l2}$ secondary phases. The typical polarization plots obtained for the AZ80 Mg samples after the open-circuit potential test for 20 min immersion in 3.5% NaCl with pH = 7 have shown in figure 10. Which can provide enhanced corrosion resistance of the ultra-fine grained AZ80 Mg alloys against Cl^- and corrosion inhibition accomplished due to obtained UFG structure in bulk material [34]. The UFG sample also shows decreased corrosion current density, Icorr compared to other samples. The polarization curves for as-received, ECAPed, MDF processed and MDF + ECAP processed AZ80 Mg alloys are presented in figure 11. The polarization curves for MDF-6P processed and MDF + ECAP processed Mg alloys exhibited similar behaviour of corrosion resistance. That means the processing with MDF and MDF followed by ECAP of Mg alloys produced a diminution of the rate of corrosion. However, the grain refinement and uniform distribution of secondary phases ($Mg_{17}Al_{12}$) induce a shift of the corrosion potential (Ecorr) towards the noble side and Also, MDF-3P followed by ECAP-2P alloy showed more defined nobler potential compared to MDF-6P + ECAP-2P processed Mg alloy. This may be due to increased dislocation densities and texture effect [35] and they are passivated by obtaining an ultra-fine grained structure. The MDF followed by ECAP samples has much smaller Icorr (table 1), value than the ECAPed, MDF and as-received sample and thereby shows reduced corrosion rate

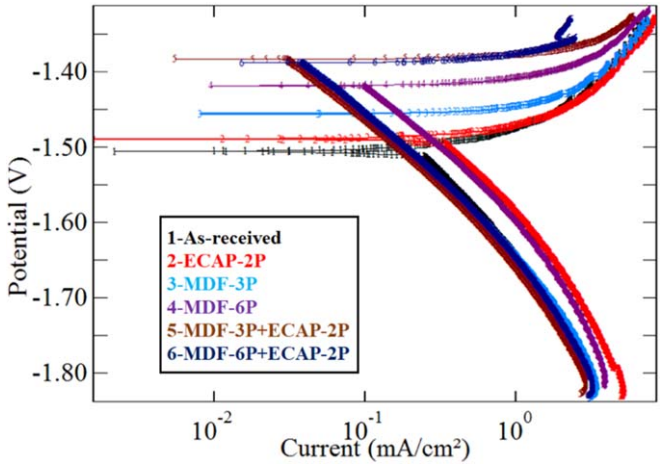

Figure 11. Corrosion behaviour of AZ80 Mg alloy: Polarization Plot.

Table 1. Potentiodynamic polarization test results.

	As-received	ECAP-2P	MDF-3P	MDF-6P	MDF-3P + ECAP-2P	MDF-6P + ECAP-2P
Ecorr (V)	−1.506	−1.491	−1.454	−1.418	−1.382	−1.389
Icorr(mA cm^{-2})	0.291	0.234	0.095	0.078	0.0	0.039
CR(mm y^{-1})	13.289	10.686	4.338	3.562	0.776	1.781

during polarization test (table 1). Further, the corrosion rate was increased after processing with MDF-6P + ECAP-2P, which was showed the inverse relationship between the corrosion rate and grain refinement due to large dislocation densities this hinders the corrosion resistance [36–38]. Figure 12 shows the corrosion morphologies of the processed and unprocessed AZ80 samples after the potentiodynamic polarization test in 3.5wt% NaCl solution. Current study evidently observed the effect of grain refinement through corrosion morphology and it has shown good promise with the experimental data.

Figure 12(a) shown the corrosion attack on the as-received sample which clearly depicts the grain boundary attacks in the unprocessed sample due to lower passivation resistance. But, SPD processed samples exhibited minimum corrosion attacks compared to the as-received Mg alloy presented in figures 12(b)–(d). Conversely, single SPD processed Mg alloy exhibited poor corrosion resistance and higher susceptibility to pitting corrosion when compared to combined processes of SPD depicts in figures 12(e) and (f). Uniformly distributed $Mg_{17}Al_{12}$ and refined grains after combined SPD (MDF + ECAP) processing led to an enhancement in the corrosion resistance and more passivated towards pitting corrosion, which is covered by thick and white corrosion products as shown in figures 12(e) and (f) and EDS result confirms that the corrosion product is $Mg(OH)_2$. Therefore, the refinement of the grains and distribution of second phase particles during severe plastic deformation processing plays a major role in corrosion resistance which is confirmed through corrosion morphology studies shown in figure 12.

4. Conclusions

The effects of MDF, ECAP and the combination of both processes on the microstructure, mechanical properties and corrosion behaviour of Mg-8%Al-0.5%Zn alloy have been investigated.

1. The microstructure of processed magnesium alloys revealed refined grains with reduced grain size. Also, it is revealed that processing with MDF followed by ECAP is an effective method to obtain well-equiaxed, homogeneous and uniform grain distribution with ultra-fine grain sizes.
2. MDF followed by ECAP can effectively refine the microstructure of AZ80 Mg alloy and improve its mechanical and corrosion properties compared to as-received, MDF and ECAP processed samples, the grain size of MDF-6P + ECAP-2P samples is reduced from 50.20 μm to ~1.29 μm, the YS, UTS and % elongation are improved from 168 MPa, 189 MPa and 3.2% to 257 MPa, 352 MPa and 11% increased by

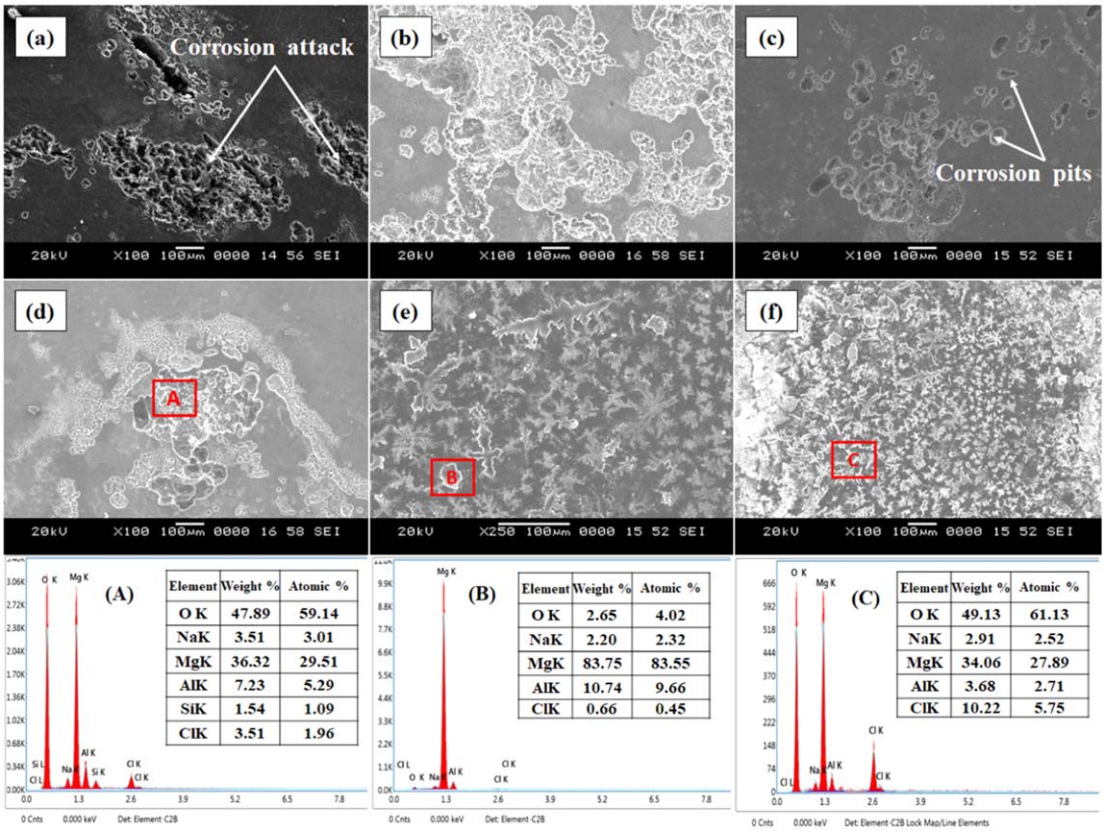

Figure 12. Corrosion morphology of AZ80 Mg alloys (a) As-received (b) ECAP-2P (c) MDF-3P (d) MDF-6P with EDS (e) MDF-3P + ECAP-2P with EDS (f) MDF-6P + ECAP-2P with EDS.

34%, 46% and 70% respectively. Initially, as-received Mg alloy showed a brittle type of fracture, but further processing to a higher number of passes lead to a mixed mode of fracture.

3. The MDF + ECAP produced UFG Mg alloy revealed enhanced corrosion resistance in 3.5 wt% NaCl solution, compared with initial as-received Mg alloy. Corrosion current density (Icorr) decreased from 0.291 mA cm^{-2} for coarse-grained Mg alloy to 0.017 mA cm^{-2} for fine-grained Mg alloys. Enrichment of corrosion resistance could be caused by grain refinement and uniform distribution of secondary phases.

Acknowledgments

This work was supported by DRDO-NRB, Government of India, under grant number NRB/4003/PG/366.

ORCID iDs

Gajanan M Naik https://orcid.org/0000-0001-9975-4096
B N Anjan https://orcid.org/0000-0002-8004-9861

References

[1] Wen K, Liu K, Wang Z, Li S and Du W 2015 *J. Magnes. Alloy* **3** 23–8
[2] Miura H, Kobayashi M and Benjanarasuth T 2016 *Mater. Trans.* **57** 1418–23
[3] Anjan B N and Preetham Kumar G V 2018 *Mater. Res. Express* **5** 106523
[4] Anjan B N and Preetham Kumar G V 2019 *Trans. Indian Inst. Met* 1–5
[5] Zhu Q, Li L, Zhang Z, Zhao Z, Zuo Y and Cui J 2014 *Mater. Trans.* **55** 270–4
[6] Hong M, Wu D, Chen R S and Du X H 2014 *J. Magnes. Alloy* **2** 317–24
[7] Salandari-Rabori A, Zarei-Hanzaki A, Fatemi S M, Ghambari M and Moghaddam M 2017 *J. Alloys Compd.* **693** 406–13
[8] Huang H and Zhang J 2016 *Mater. Sci. Eng.* A **674** 52–8
[9] Zhang J, Xie H, Lu Z, Ma Y, Tao S and Zhao K 2018 *Results in Physics* **10** 967–72
[10] Avvari M, Narendranath S and Shivananda Nayaka H 2015 *Int. J. Mater. Prod. Technol. Mater. Prod. Technol.* **51** 139–64
[11] Naik G M, Gote G D and Narendranath S 2018 *Mater. today: Proc.* **5** 17763–8

[12] Avvari M, Narendranath S and Able M 2016 *Adv. Mech. Eng.* **8** 168781401665182
[13] Gopi K R and Shivananda Nayaka H 2017 *J. Mater. Res.* **32** 2153–60
[14] Zhou L, Liu Y, Zhang J and Kang Z 2016 *Mater. Sci. Technol.* **32** 969–75
[15] Liao Q, Chen X, Lan Q, Ning F and Le Q 2018 *Mater. Res. Express* **5** 126510
[16] Zhao L, Ma G, Jin P, Li X and Yu Z 2018 *Mater. Res. Express* **6** 036524
[17] Heczel A, Akbaripanah F, Salevati M A, Mahmudi R, Vida A and Gubicza J 2018 *J. Alloys Compd.* **763** 629–37
[18] Shakhova I, Belyakov A and Kaibyshev R 2014 *IOP Conf. Ser. Mater. Sci. Eng.* **63** 012097
[19] Naik G M, Gote G D, Narendranath S and Satheesh Kumar S S 2018 *Mater. Res. Express* **5** 086513
[20] Suresh K, Rao K, Prasad Y, Wu C M, Hort N and Dieringa H 2017 *Metals* **7** 539
[21] Arab S M and Akbarzadeh A 2014 *J. Magnes. Alloys* **2** 203–7
[22] Poggiali F S J, Silva C L P, Pereira P H R, Figueiredo R B and Cetlin P R 2014 *J. Mater. Res. Technol.* **3** 331–7
[23] Zhao G, Fan J, Zhang H, Zhang Q, Yang J, Dong H and Xu B 2018 *Mater. Sci. Eng.* A **731** 54–60
[24] Zeng R C, Qi W C, Zhang F and Li S Q 2016 *Regenerative Biomaterials* **3** 49–56
[25] Yu H, Xin Y, Wang M and Liu Q 2018 *J. Mater. Sci. Technol.* **34** 248–56
[26] Jiang L, Huang W, Zhang D, Guo F, Xue H, Xu J and Pan F 2017 *J. Alloys Compd.* **727** 205–14
[27] Shaeri M H, Shaeri M, Ebrahimi M, Salehi M T and Seyyedein S H 2016 *Prog. Nat. Sci.: Mater. Inter.* **26** 182–91
[28] Suresh M, Sharma A, More A M, Kalsar R, Bisht A, Nayan N and Suwas S 2019 *J. Alloys Compd.* **785** 972–83
[29] Torkian A, Faraji G and Karimpour M 2018 *Arch. Metall Mater.* **63** 1094–100
[30] Duley P, Sanyal S, Bandyopadhyay T K and Mandal S 2019 *Mater. Des.* **164** 107554
[31] Kim W J, Hong S I, Kim Y S, Min S H, Jeong H T and Lee J D 2003 *Acta Mater.* **51** 3293–307
[32] Del Valle J A, Carreño F and Ruano O A 2006 *Acta Mater.* **54** 4247–59
[33] Avvari M and Able M 2016 *Adv. Mech. Eng.* **8** 1687814016651820
[34] Jiang B, Xiang Q, Atrens A, Song J and Pan F 2017 *Corros. Sci.* **126** 374–80
[35] Song G L 2012 *JOM* **64** 671–9
[36] Naik G M, Gote G D, Narendranath S and Satheesh Kumar S S 2018 *Adv. Mater. Res.* **7** 105–18
[37] Naik G M, Narendranath S and Kumar S S 2019 *J. of Materi. Eng. and Perform.* **28** 2610–2619
[38] Gajanan M N, Narendranath S and Satheesh Kumar S S 2019 *AIP Conf. Proc.* **2082** 030016